most intense crystal field absorptions in most coordinations expected in the mantle are in the near infrared. This is a spectral region that cannot be studied by the present spectrographic system, and so the effects of large compressions on the absorption spectrum of single-crystal ruby ($Cr^{3+}:Al_2O_3$), which is in a spectral region accessible to the system, were studied instead. We believe that the behavior of $Fe^{2+}$ can be inferred from such data by using techniques such as those of *Gaffney* [1972]. The corundum ($Al_2O_3$) structure is, of course, a close analog to the ilmenite structure. This structure is probably the form in which the pyroxene and garnet minerals exist in a major part of the lower mantle. The present experiments span the range from 147 to 530 kb. The highest pressure is more than three times greater than the maximum attained in static compression experiments on corundum [*Stephens and Drickamer,* 1961]. Such measurements permit a determination of the local environment about the $Cr^{3+}$ impurities in the corundum ($Al_2O_3$) lattice. The data are presented below and discussed in light of the hydrostatic spectral studies and the recent Hugoniot measurements on sapphire [*Graham and Brooks,* 1971].

The principal absorptions in ruby arise from the $Cr^{3+}$ ion's substituting in Al sites in corundum. These sites are nearly octahedral with some trigonal distortion. In the pure octahedral field the $^4F$ ground state of $Cr^{3+}$ splits into $^4A_2$, $^4T_2$, and $^4T_1$ [*Tanabe and Sugano,* 1956]. The observed absorptions in the visible correspond to the electronic transitions $^4A_2 \rightarrow {}^4T_2$ at about 18,000 $cm^{-1}$ and $^4A_2 \rightarrow {}^4T_1$ at about 25,000 $cm^{-1}$. The trigonal field splits the excited state $^4T_2$ into $^4A_1$ and $^4E$ states and the state $^4T_1$ into $^4A_2$ and $^4E$ states with separations of about 500 $cm^{-1}$, but this is too small (relative to the widths of the absorptions) to be determined in the unpolarized spectra reported here [*Stephens and Drickamer,* 1961, Figure 1].

The effect of hydrostatic pressures up to 150 kb on the spectra of ruby has been studied by *Stephens and Drickamer* [1961]. They found that $Dq$ increased proportional to $1/r^5$ as $r$, the mean interatomic distance, decreased. This is exactly the behavior predicted for a point charge model [*Gaffney,* 1972]. Since Stephens and Drickamer measured the positions of both the $^4A_2 \rightarrow {}^4T_2$ and $^4A_2 \rightarrow {}^4T_1$ transitions up to 120 kb, they were also able to determine that one of the Racah parameters ($B$) decreases on compression approximately as $r^3$. (There is no model for predicting the change of $B$ or $C$ with interatomic distance.) From the polarization dependence of the spectra they found that the trigonal splitting of the $^4T_2$ and $^4T_1$ states increased on compression for pressures over 60 kb. The value extrapolated from 120 to 150 kb would be about 950–1000 $cm^{-1}$. It was not possible in our experiments to determine the variation of the Racah parameters in ruby at larger compressions because the spectrograph could not follow the position of the $^4A_2 \rightarrow {}^4T_1$ transition into the shocked region as a result of the spectral sensitivity of the streak camera photocathode.

The samples studied here were single-crystal pink ruby (0.5% $Cr:Al_2O_3$) disks 6 mm thick and 22 mm in diameter with the crystallographic $c$ axis at 60° to the flat surfaces. They were flat to one wave and polished with one surface aluminized. Fabrication was done by the vendor, Union Carbide, Crystal Products Division. An unpolarized absorption spectrum of one of the samples taken at room temperature is shown in Figure 9.

Spectra were measured at three values of normal shock stress, one below the elastic limit (147 kb) and two above (430 and 530 kb). The data obtained from these three experiments are summarized in Table 2. Figure 10 shows a typical photographic record. These photographic negatives were digitized and stored on tape by the Image Processing Laboratory of the Jet Propulsion Laboratory and then computer processed to reduce the noise level.

To obtain the positive of the absorption peaks under shock compression, microdensitometer traces across the film were differenced to show the change in the absorption between two traces, one taken in the low-pressure region (of the film) and the other taken in the high-pressure region. If the earlier trace is subtracted from the later one, absorption maximums in the low-pressure region appear as negative features, whereas those in the high-pressure region will be positive features.

To evaluate the results summarized in Table 2, one must distinguish between absorptions in the volumes ahead of and behind the shock front, on the one hand, and at interfaces such

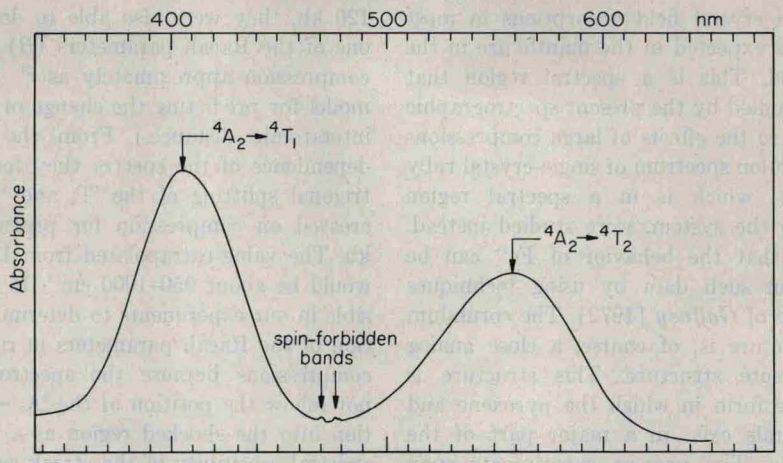


Fig. 9. Absorption spectrum of pink ruby ($Al_2O_3$:0.05% $Cr_2O_3$) at zero pressure.

as the internal mirror, the shock front, and the free surfaces on the other. In principle, this is easy to do, since the former will have intensities that vary with time, whereas the latter will not vary during the experiment. In practice, it is often difficult to make such a decision because the signal-to-noise ratio is so low that it is difficult to obtain meaningful information about intensities. In the present case the highest energy absorption observed at 147 kb was time invariant, so that one can conclude that either the elastically shocked mirror or the elastic front produces this feature. This feature is not observed in the other spectra.

The energy of the $^4A_2 \rightarrow {}^4T_2$ transition is just 10 $Dq$, and so we can plot the data of Table 2 against relative volume as determined by *Graham and Brooks* [1971] to determine the variation of $Dq$ with interatomic distance (Figure 11). There are two distinct regions of behavior. Below the Hugoniot elastic limit (HEL) there are very great nonhydrostatic stresses. On the basis of the discussion by Graham and Brooks, the difference in principal stresses behind the shock front at 147 kb normal stress is about 90 kb. It is to be expected, therefore, that the local symmetry about the $Cr^{3+}$ ions is considerably distorted from that of the octahedral case. This distorted symmetry is exactly what is found below the HEL. The usually triply degenerate absorption due to $^4A_2 \rightarrow {}^4T_2$ is split by more than 3730 $cm^{-1}$, almost four times the value extrapolated from hydrostatic experiments.

Above the HEL we find a very different situation. Now there is only one absorption discernible, indicating that the splitting of the $^4T_2$ state due to nonoctahedral fields is less than about 800 $cm^{-1}$. (The absorption due to the elastically shocked region is not discernible because at any given moment less than 20% of the material behind the elastic shock is ahead of the second shock. The shock velocities for the elastic and second waves are about 11 and 9 mm/sec, respectively.) This means that the strain must be nearly isotropic at stresses of the order of 400–500 kb and therefore that the nonhydrostatic component of stress must be fairly small. If the splitting of $^4A_2 \rightarrow {}^4T_2$ band

TABLE 2. Spectral Data for Ruby

| Shock Pressure, kb | Absorption Band, nm | Assignment |
|---|---|---|
| 0 | 559* | $^4A_2 \rightarrow {}^4F$¶ |
| | 546* | $^4A_2 \rightarrow {}^4A_1$" |
| 147 ± 3 | 478 ± 5† | $^4A_2 \rightarrow {}^4T_2$† |
| | 524 ± 10† | |
| | 581 ± 4† | |
| | 446 ± 3§ | |
| 430 ± 10 | 460 ± 10 | $^4A_2 \rightarrow {}^4T_2$ |
| 530 ± 10 | 411 ± 12 | $^4A_2 \rightarrow {}^4T_2$ |

*Stephens and Drickamer* [1961].
†Triple degeneracy removed by nonhydrostatic strain around $Cr^{+3}$ site.
§Time invariant absorption arising from either shock front or reflecting mirror.
¶Perpendicular to $c$ axis.
"Parallel to $c$ axis.